



OPEN ACCESS

EDITED BY

Khan M. G. Mostofa,
Tianjin University, China

REVIEWED BY

Ralf Schiebel,
Max Planck Society, Germany
Franck Bassinot,
UMR8212 Laboratoire des Sciences du
Climat et de l'Environnement
(LSCE), France

*CORRESPONDENCE

Helge A. Winkelbauer
✉ helge.winkelbauer@gmail.com
Babette A. A. Hoogakker
✉ b.hoogakker@hw.ac.uk

SPECIALTY SECTION

This article was submitted to
Marine Biogeochemistry,
a section of the journal
Frontiers in Marine Science

RECEIVED 11 November 2022

ACCEPTED 23 January 2023

PUBLISHED 02 February 2023

CITATION

Winkelbauer HA, Hoogakker BAA,
Chance RJ, Davis CV, Anthony CJ,
Bischoff J, Carpenter LJ, Chenery SRN,
Hamilton EM, Holdship P, Peck VL,
Poulton AJ, Stinchcombe MC and
Wishner KF (2023) Planktic foraminifera
iodine/calcium ratios from plankton tows.
Front. Mar. Sci. 10:1095570.
doi: 10.3389/fmars.2023.1095570

COPYRIGHT

© 2023 Winkelbauer, Hoogakker, Chance,
Davis, Anthony, Bischoff, Carpenter,
Chenery, Hamilton, Holdship, Peck,
Poulton, Stinchcombe and Wishner. This is an open-
access article distributed under the terms of
the [Creative Commons Attribution License
\(CC BY\)](https://creativecommons.org/licenses/by/4.0/). The use, distribution or
reproduction in other forums is permitted,
provided the original author(s) and the
copyright owner(s) are credited and that
the original publication in this journal is
cited, in accordance with accepted
academic practice. No use, distribution or
reproduction is permitted which does not
comply with these terms.

Planktic foraminifera iodine/calcium ratios from plankton tows

Helge A. Winkelbauer^{1*}, Babette A. A. Hoogakker^{1*},
Rosie J. Chance², Catherine V. Davis³, Christopher J. Anthony²,
Juliane Bischoff¹, Lucy J. Carpenter², Simon R. N. Chenery⁴,
Elliott M. Hamilton⁴, Philip Holdship⁵, Victoria L. Peck⁶,
Alex J. Poulton¹, Mark C. Stinchcombe⁷ and Karen F. Wishner⁸

¹Lyell Centre for Earth and Marine Science and Technology, Heriot-Watt University, Edinburgh, United Kingdom, ²Wolfson Atmospheric Chemistry Laboratories, Department of Chemistry, University of York, York, United Kingdom, ³Department of Marine, Earth, and Atmospheric Sciences, North Carolina State University, Raleigh, NC, United States, ⁴Inorganic Geochemistry, Centre for Environmental Geochemistry, British Geological Survey, Environmental Science Centre, Nottingham, United Kingdom, ⁵Department of Earth Sciences, University of Oxford, Oxford, United Kingdom, ⁶BAS-Arctic Working Group, British Antarctic Survey, Cambridge, United Kingdom, ⁷National Oceanography Centre, Ocean BioGeosciences, Southampton, United Kingdom, ⁸Graduate School of Oceanography, University of Rhode Island, Narragansett, RI, United States

Planktic foraminifera test iodine to calcium ratios represent an emerging proxy method to assess subsurface seawater oxygenation states. Several core-top studies show lower planktic foraminifera I/Ca in locations with oxygen depleted subsurface waters compared to well oxygenated environments. The reasoning behind this trend is that only the oxidized species of iodine, iodate, is incorporated in foraminiferal calcite. The I/Ca of foraminiferal calcite is thought to reflect iodate contents in seawater. To test this hypothesis, we compare planktic foraminifera I/Ca ratios, obtained from plankton tows, with published and new seawater iodate concentrations from 1) the Eastern North Pacific with extensive oxygen depletion, 2) the Benguela Current System with moderately depleted oxygen concentrations, and 3) the well oxygenated North and South Atlantic. We find the lowest I/Ca ratios (0.07 $\mu\text{mol/mol}$) in planktic foraminifera retrieved from the Eastern North Pacific, and higher values for samples (up to 0.72 $\mu\text{mol/mol}$) obtained from the Benguela Current System and North and South Atlantic. The I/Ca ratios of plankton tow foraminifera from environments with well oxygenated subsurface waters, however, are an order of magnitude lower compared to core-tops from similarly well-oxygenated regions. This would suggest that planktic foraminifera gain iodine post-mortem, either when sinking through the water column, or during burial.

KEYWORDS

I/Ca, planktic foraminifera, plankton nets, oxygen concentration, oxygen proxy

Introduction

Ocean deoxygenation caused by global warming poses a major threat to the sustainability of fisheries and marine ecosystems, as well as key global biogeochemical cycles (Breitburg et al., 2018). Oxygen minimum zones (OMZs) are predicted to expand dramatically by 2100 (Oschlies et al., 2008). Being able to trace the existence of past OMZs, using sedimentary proxies, is crucial to understand OMZ dynamics and improve future predictions.

The chemical speciation of redox active elements such as iodine often reflects seawater oxygen levels – iodine in the oceans exists predominantly as iodide (I^-) and iodate (IO_3^-), with the former being dominant in anoxic environments (Wong and Brewer, 1977; Wong et al., 1985; Rue et al., 1997; Truesdale and Bailey, 2000). Planktic foraminifera are ubiquitous microorganisms that incorporate iodate into their calcite shells (Lu et al., 2016b). Due to the broad dependency of iodine speciation on seawater oxygen levels, iodine to calcium ratios (I/Ca) in planktic foraminifera may be a promising tool to assess the oxygenation state of the seawater that they calcified in. Use of I/Ca in carbonates as a paleo tracer for ocean oxygen levels primarily depends on the iodate concentration in seawater; abiotic calcite synthesis experiments suggest that iodate is the preferred iodine species taken up into calcite, and that the amount incorporated reflects concentrations in seawater (Lu et al., 2010; Zhang et al., 2013). Synchrotron X-ray absorption spectroscopy and first-principles calculations confirm that iodate ions substitute for

carbonate ions in the calcite crystal lattice (Podder et al., 2017; Feng and Redfern, 2018). However, this needs to be further tested in the natural marine environment on living foraminifera.

Limited observations from oxygen-depleted environments such as the Eastern Tropical South Pacific or Gulf of Mexico do not show a clear trend when comparing surface water iodate concentrations from areas with suboxia ($O_2 < 10 \mu\text{mol/kg}$) to those from similar latitudes lacking suboxia (Figure 1). Planktic foraminifera from sediment core-tops ($< 5,000$ years) from areas with extensive suboxia have very low I/Ca ratios ($< 1 \mu\text{mol/mol}$), compared with those from well-oxygenated regions (I/Ca ratios $> 4 \mu\text{mol/mol}$) (Lu et al., 2016a), which is thought to coincide with lower seawater iodate concentrations. Recent applications of proxy I/Ca ratios have shed new light on glacial subsurface water oxygen concentrations, suggesting that the Pacific sector of the Southern Ocean was oxygen depleted during glacial times (Lu et al., 2016a), with tandem downward expansion of the Eastern Tropical North Pacific (ETNP) OMZ (Hoogakker et al., 2018). Currently the planktic foraminifera I/Ca proxy can only be applied qualitatively, as we do not have a clear mechanistic understanding of iodine incorporation into the calcite.

Until now I/Ca calibration studies have focused on recent (< 5000 years) sediment core-tops, but not on fresh foraminifera from plankton nets. We do not know what seawater iodate concentrations core-top foraminifera calcified in. This leaves uncertainties as to what extent shell I/Ca is directly proportionate to seawater iodate. Core-top measurements from areas with an

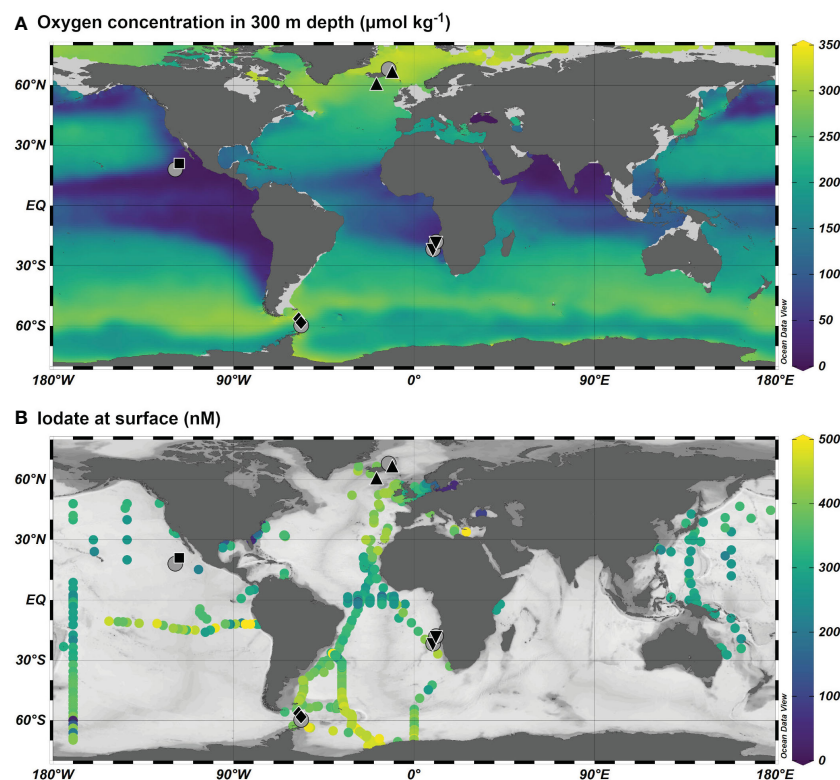


FIGURE 1

Station map for plankton tows (black, see Table 1) and iodate profiles (grey circles) from Moriyasu et al. (2020) in the Pacific, Bluhm et al. (2011) in the Southern Ocean, Waite et al. (2006) in the North Atlantic and from this study in the Benguela Upwelling System. (A) Average oxygen concentration at 300 m from the World Ocean Atlas 2018 (Garcia et al., 2019). (B) Iodate concentration at the surface (< 15 m) from the compilation described in Chance et al. (2014), plus Cutter et al. (2018) and Moriyasu et al. (2020) (dataset available: <https://www.bco-dmo.org/dataset/776552>). Plotted using Ocean Data View (Schlitzer, 2022).

extensive OMZ show consistently low I/Ca <2.5 $\mu\text{mol/mol}$ for both mixed layer species and deeper dwellers (Lu et al., 2016a; Hoogakker et al., 2018; Lu et al., 2020). Observations show that the well-oxygenated mixed layer above the OMZ contains iodate, whilst the deeper anoxic waters generally do not (Rue et al., 1997; Cutter et al., 2018; Moriyasu et al., 2020). This leaves the conundrum of why in certain locations mixed layer planktic foraminifera species show low I/Ca ratios as do the deeper dwelling species.

To assess the extent to which seawater iodate is incorporated in planktic foraminifera shells we present I/Ca measured from the shells of foraminifera caught in plankton tows. This includes samples from the tropical Northeast Pacific, with an intense OMZ, samples from the Benguela area, with a weakly developed OMZ, and samples from the North and South Atlantic with a well-oxygenated water column. We compare these planktic foraminifera I/Ca ratios with published (Pacific, North and South Atlantic) and novel (Benguela) water column iodate and dissolved oxygen measurements.

Locations

Eastern Tropical North Pacific OMZ

The Eastern Tropical North Pacific has one of the worlds' largest OMZs, and contains very depleted O_2 levels (minimum between 2

and 10 $\mu\text{mol/kg}$ at ~430 m water depth; Wishner et al., 2018). Coastal upwelling causes high productivity and high sinking fluxes of organic matter to depth. Accumulation of nitrite in subsurface waters is indicative of nitrate reduction (Garfield et al., 1983; Buchwald et al., 2015; Medina Faull et al., 2020). The sample area is located offshore, away from the upwelling and high productivity, though nevertheless it is characterized by low oxygen as a result of low oxygen waters moving away from the coast and poorly ventilated intermediate waters in the ETNP (Table 1). Within the core of the OMZ, oxygen levels reach 2 $\mu\text{mol/kg}$. The depth of the upper boundary of the OMZ in the area varies between ~ 100 and 130 m. Like its South Pacific counterpart, it is thought that there is lateral input of excess iodide-iodine from the sedimentary margins (Cutter et al., 2018; Moriyasu et al., 2020).

Benguela current

The Benguela Current is an eastern boundary current, which flows north along the coast of South Africa and Namibia until it meets warm southward flowing equatorial surface currents between 15.5° S and 17° S (Veitch et al., 2006). The location of the Angola-Benguela front that separates northward and southward flowing waters changes seasonally. Upwelling along the coast introduces nutrients to the

TABLE 1 Sample details, locations and I/Ca values of plankton net samples.

Location	Name/Event	Latitude	Longitude	Species	Water depth (m)	I/Ca ($\mu\text{mol/mol}$)
Eastern North Pacific OMZ	SKQ2017_721_6+7+8+9	21.55°N	117.80°W	<i>T. sacculifer</i>	125 to surface	*
Eastern North Pacific OMZ	SKQ2017_726_4+7	21.55°N	117.80°W	<i>T. sacculifer</i>	~ 430 \pm 5	0.09
Eastern North Pacific OMZ	SKQ2017_726_6	21.55°N	117.80°W	<i>O. universa</i>	~ 430 \pm 5	0.07
Eastern North Pacific OMZ	SKQ2017_726_6+8	21.55°N	117.80°W	<i>Globigerinella siphonifera</i>	~ 430 \pm 5	0.17
Eastern North Pacific OMZ	SKQ2017_726_7	21.55°N	117.80°W	<i>O. universa</i>	~ 430 \pm 5	0.07
Eastern North Pacific OMZ	SKQ2017_726_8	21.55°N	117.80°W	<i>O. universa</i>	~ 430 \pm 5	0.07
Benguela Current SB	DY090 #07/ E96	21.56°S	9.47°E	<i>G. menardii</i>	120 to surface	0.33
Benguela Current NB	DY090 #13/ E189	18.02°S	11.01°E	<i>G. menardii</i>	120 to surface	0.33
Benguela Current NB	DY090 #14/ E190	18.02°S	11.01°E	<i>G. inflata</i>	750 to 500	0.53
Benguela Current NB	DY090 #17/ E190	18.02°S	11.01°E	<i>G. inflata</i>	120 to surface	0.72
Benguela Current NB	DY090 #17/ E190	18.02°S	11.01°E	<i>G. inflata</i>	120 to surface	0.48
Benguela Current NB	DY090 #18/ E214	18.03°S	11.01°E	<i>G. inflata</i>	120 to surface	0.55
North Atlantic	JR271 B5	60°N	18.67°W	<i>G. bulloides</i>	200 to surface	0.34
North Atlantic	JR271 B6	65.98°N	10.72°W	<i>N. pachyderma</i>	200 to surface	0.38
S Atlantic	JR274 B1	56.47°S	57.43°W	<i>G. bulloides</i>	200 to surface	0.65
S Atlantic	JR274 B1	56.47°S	57.43°W	<i>G. bulloides</i>	200 to surface	0.19
S Atlantic	JR274 B3	58.37°S	56.25°W	<i>N. pachyderma</i>	200 to surface	0.3

*Below detection limit.

SB, South Benguela; NB, North Benguela.

photic zone, causing high primary productivity. Decomposition of this organic material results in modest depletion of sub-surface oxygen levels.

Both sampling locations (Table 1) are in the northern half of the Benguela system, but south of the Angola-Benguela Front. The mixed layer depth during the sampling (MLD) at the offshore site South Benguela (SB) was 50 m with a surface water temperature of 20.6°C (Figure 1). The surface water at the site North Benguela (NB) was 2.8°C colder with a variable MLD between 15 m and 45 m during the sampling period. Oxygen values were slightly lower at NB than SB with a minimum of 25 $\mu\text{mol/kg}$ at 300 m (compared to 41 $\mu\text{mol kg}^{-1}$ at SB at 420 m). The main difference between sites was the much shallower onset of oxygen-depleted waters just below the surface mixed layer at NB, as opposed to at a depth of ~ 120 m in SB. South Benguela displayed a typical low-nutrient tropical open ocean chlorophyll-a profile with a subsurface maximum of 0.4 mg/m^3 at 70 m depth. In contrast, NB had a surface chlorophyll-a maximum with an average of 1 mg/m^3 .

North and South Atlantic Ocean

The North and South Atlantic samples represent well-oxygenated water masses which do not have dissolved oxygen concentrations below 235 $\mu\text{mol/kg}$ in the upper 1000 m. The North Atlantic samples came from two sites to the south and to the east of Iceland with average SST of ca. 9°C (Table 1). Deep-water production in the Greenland and Norwegian seas causes a particularly well-ventilated water column with oxygen concentrations of 265–330 $\mu\text{mol/kg}$ (WOA18, Boyer et al., 2018).

The South Atlantic samples were from the Drake Passage through which the Antarctic Circumpolar Current flows along with its strong associated fronts (Orsi et al., 1995). The two samples are two degrees of latitude apart from each other (see Table 1 for coordinates) with SSTs of 1.7°C and 5.4°C and high oxygen concentrations in the water column of 260–330 $\mu\text{mol/kg}$ (WOA18, Boyer et al., 2018). These waters are well ventilated with Antarctic intermediate waters due to Southern Ocean overturning circulation.

Methods

Collection of samples during the cruises

Planktic foraminifera samples for the ETNP were collected using a horizontally towed 1 m^2 MOCNESS (Multiple Opening/Closing Net and Environmental Sensing System, 222 μm mesh size) at ~ 425 m for station 726 and a vertical haul from 125 m to the surface for station 721 during R/V Sikuliaq cruise SKQ201701S in Jan-Feb 2017 (Wishner et al., 2018). At sea, the samples were stored in sodium-borate-buffered seawater and formalin. Several months later they were picked and stored in dry slides.

Planktic foraminifera samples from the Benguela Current were collected during research cruise DY090 aboard the RRS Discovery in May to June 2018 using vertical hauls of Bongo nets and a MultiNet[®] Mammoth with 100 μm mesh size. Most nets sampled the upper 120 m of the water column, but one sample was from a depth of 750 m to

500 m. Samples were washed from the net into a bucket with surface seawater. Following gravitational settling, planktic foraminifera were collected from the bottom of the bucket using a hand pipette. Foraminifera were washed over a 100 μm mesh with pH-adjusted Milli-Q (ammonia solution, pH > 8), and oven dried (40 to 50°C, 8–12 h) before storage.

Samples from two stations in the well-oxygenated high latitude North Atlantic (Greenland and Norwegian Seas) and two stations in the South Atlantic (Drake Passage) were collected during two research cruises (JR271 in 2012 and JR274 in 2013) as part of the UK Ocean Acidification Research Program (www.oceanacidification.org.uk). Plankton samples from vertical Bongo net hauls (200 m to surface, 100 μm mesh size) were collected, rinsed, dried, and stored in the same way as the samples from the Benguela Current.

Seawater: oxygen concentrations

For the Pacific cruise SKQ2017, oxygen data was derived from two sources: a Sea-Bird SB911 plus CTD including a SBE43 dissolved oxygen sensor attached to the MOCNESS, and a CTD with an Aanderaa 4831F oxygen sensor was attached to a Wire Flyer (towed deep oscillating profiler) (Wishner et al., 2018). The Wire Flyer and MOCNESS oxygen sensors were cross-calibrated during the cruise and by post-cruise analyses. For the Benguela cruise DY090, *in situ* oxygen data came from a Sea-Bird SBE43 dissolved oxygen sensor attached to a SBE 9plus CTD calibrated against discrete Winkler titrations using a Metrohm 716 DMS Titrino (cruise report: https://www.bodc.ac.uk/resources/inventories/cruise_inventory/reports/dy090.pdf).

Seawater iodate

During the Benguela cruise DY090 seawater samples for iodine analyses were taken from the upper 1000 m (except two CTD casts to >3500 m depth), at the same depths as discrete oxygen samples. Following collection, the samples were filtered (0.2 μm , polycarbonate Whatman Nucleopore[™] filter) under gentle vacuum, and transferred to 50 mL polypropylene screw cap tubes. Duplicate aliquots were prepared for each sample, one for iodate and the other for iodide analysis. Aliquots were frozen at -20°C for transport back to the University of York for analysis. The majority (65%) of frozen samples were analyzed within 12 months of collection, and all analyses were complete within 32 months of collection. Campos (1997) has shown that inorganic iodine speciation is preserved in filtered frozen samples ($\leq -16^\circ\text{C}$) for at least one year and Schwehr and Santschi (2003) found no significant change after three years. Iodate was determined using a spectrophotometer (UV-1800, Shimadzu) after reduction to iodonium (Truesdale and Spencer, 1974; Jickells et al., 1988), with calibration using external KIO₃ standards. Around half the samples were analyzed singly, and the other half in triplicate, due to a change in laboratory protocol. Where samples were analyzed singly, precision was estimated by propagation of error from the calibration curve. Where samples were analyzed in triplicate, precision was estimated from the standard deviation of the replicates. The precision of these measurements varied, and is shown as individual error bars on each

data point (Figure 2 and Supplementary information). Fifty percent of samples had a percentage relative standard deviation (%RSD) of less than or equal to 4%, and 92% had a %RSD below 15%. The limit of detection was approximately 50 nM. The iodate measurements from the North and South Atlantic (Waite et al., 2006; Bluhm et al., 2011) were made using the same iodometric method as our own measurements.

Planktic foraminifera I/Ca ratios

Towed planktic foraminifera I/Ca ratios were measured using a magnetic-sector ICP-MS (Thermo Finnigan Element 2 at the Department of Earth Sciences, University of Oxford) and an Agilent Technologies 8900 ICP-QQQ (British Geological Survey Keyworth). On average we used 90 specimens per analysis. As reference material we used the carbonate standard JCP-1 which is not certified as an I/Ca standard but is often used in I/Ca studies. It is a ground coral, which we measured at 4.27 ± 0.10 $\mu\text{mol/mol}$ in Oxford (n=13) and 4.82 ± 0.06 $\mu\text{mol/mol}$ in Keyworth (n=6). Previously published I/Ca ratios for the JCP-1 coral are 4.33 ± 0.16 $\mu\text{mol/mol}$ (Chai and Muramatsu, 2007), 4.27 ± 0.06 $\mu\text{mol/mol}$ (Lu et al., 2010) and 3.82 ± 0.08 $\mu\text{mol/mol}$ (Glock et al., 2014). For the Pacific samples, only dead (empty) planktic foraminifera specimens were selected, which contrasts to samples from the North and South Atlantic and the two stations in the Benguela Current System where most foraminifera were alive, with their cytoplasm present.

Prior to all analyses, samples were rinsed with ultra-pure (18.2 M Ω cm) water and treated to remove organic material. Glock et al. (2016) showed that organic material in benthic foraminifera could be a significant source of iodine. We carried out a set of experiments on core-top samples (ODP Site 1088, 0-1 cm, 41.14°S, 13.56°E, 2082 m

below sea level) to assess which method may remove organic material/iodine contamination most effectively, using A) 1% buffered H₂O₂ x 6, following Winkelbauer et al. (2021), B) 50% (v/v) buffered H₂O₂ for 30 minutes (Anand et al., 2003), C) soaking in bleach, and D) combustion at 450 °C. Before measuring I/Ca ratios in planktic foraminifera each sample was initially rinsed in ultra-pure de-ionized water. We assume that the cleaning method resulting in the lowest planktic foraminifera I/Ca ratios, was the most adequate at removing organic material within and adhered to the foraminifera tests. Overall, the method of Winkelbauer et al. (2021), using 1% (v/v) buffered H₂O₂ acquires the lowest I/Ca result, whereas the method using bleach showed the highest value (Table 2). We therefore used the method of Winkelbauer et al. (2021) to remove organic material, which involved six repetitions of soaking the crushed samples in buffered 1% (v/v) H₂O₂ at boiling point for ten minutes. The same sample from ODP 1088, 0-1 cm was also used to measure planktic foraminifera with different preservation states, i.e., semi-transparent tests and fully opaque encrusted tests.

Results

Figure 2 shows a generalized overview of seawater dissolved oxygen and iodate concentrations for the different locations. For the Eastern Tropical North Pacific, we show water column data from station F19 (Falkor cruise FK 180624) obtained by Moriyasu et al. (2020), which is 400 km away from our plankton tow location. At this location dissolved oxygen concentrations (~200 $\mu\text{mol/kg}$) were uniform in the top 80 m and then decrease to almost 0 $\mu\text{mol/kg}$ at 140 m water depth and deeper in the water column (Figure 2D). Between 0 and 110 m water depth iodate concentrations at this location vary between ~250 and 330 nmol/l, decreasing to < 50 nmol/l until ~ 210 m after which they increased to >400 nmol/l (Figure 2A).

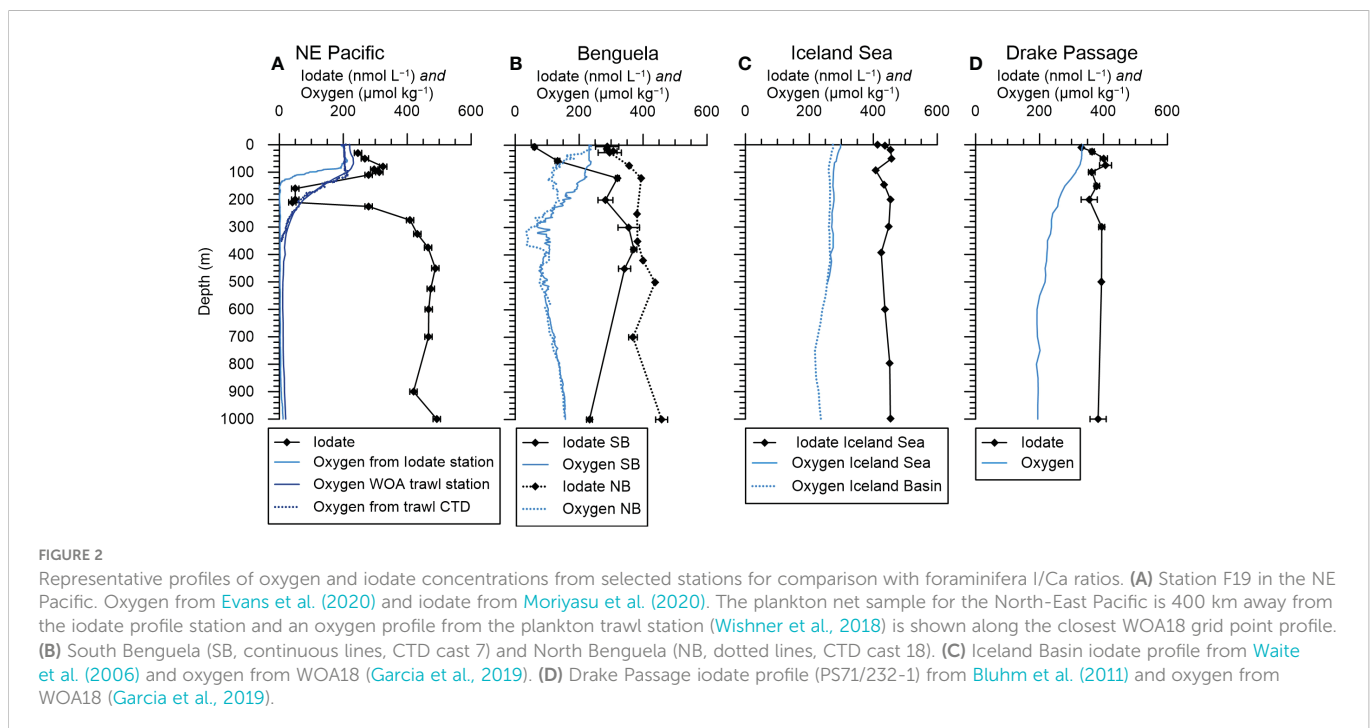


TABLE 2 Effect of different organic material removal techniques on core-top sample from ODP 1088 (0-1 cm, > 300 μm *Globigerina bulloides*).

Sample	Organic carbon removal treatment	I/Ca in $\mu\text{mol/mol}$
A1	Buffered 1% H_2O_2	4.2
A2*	Buffered 1% H_2O_2	3.9
B1	Buffered 50 % H_2O_2	4.0
B2	Buffered 50 % H_2O_2	5.0
C1	Soaking in bleach (4 hours)	5.9
C2	Soaking in bleach (4 hours)	5.3
D1	Combustion at 450 °C	4.7
D2	Combustion at 450 °C	4.4

*Was stabilized using tetramethylammonium hydroxide but cleaned using the same method. For a comparison of stabilization techniques please refer to Winkelbauer et al. (2021).

At the Benguela location, the SB station had a mixed layer with oxygen concentrations of 232–218 $\mu\text{mol/kg}$ between 0 and 120 m (Figure 2B). At the North Benguela station there is a two-step decrease in dissolved oxygen from the surface with 237 $\mu\text{mol/kg}$ to 310 m where the lowest dissolved oxygen concentrations of ~ 35 $\mu\text{mol/kg}$ occurred (Figure 2B).

Iodate concentrations were variable over time at both stations in the Benguela Current System, and the closest CTD casts to the net hauls are shown in Figure 2B. At SB, the CTD and bottle sampling was ca. 40 hours before the net hauls and at NB all net samples were taken within 32 h before or after the CTD and bottle sampling. At both stations the iodate concentration increased from the surface to 120 m depth, though the water samples from SB had lower concentrations going from 60 nmol/l to 320 nmol/l while NB had concentrations from 226 nmol/l to 400 nmol/l (Figure 2B). Water samples from four days earlier (CTD 1) at SB had higher iodate concentrations in the top 120 m, ranging from 230 to 300 nmol/l. Comparable depletions of iodate in low latitude surface waters have been observed elsewhere in the Atlantic, and are attributed to a combination of biological activity and stratification (e.g., Campos et al., 1996; Truesdale et al., 2000). The extent of the depletion seen in CTD 7 is particularly large, and the change over four days rapid given the relatively slow rates of iodine transformations (see e.g., Chance et al., 2014). We suggest this could be due to advection of a localized area of particularly high biological activity near the station. The two CTDs 1 and 7 are also ca. 40 km apart from each other and therefore reflect local variation in surface iodate distribution (see Supplementary Table 1 for exact locations and times of the CTDs). In the deeper water, below 120 m, the iodate concentrations were also always lower at SB than at NB despite oxygen concentrations being similar. This may result from the slow iodine oxidation kinetics and highlights that iodate concentrations are not solely a function of oxygen level. All iodate and oxygen profiles are shown in supplementary Figures 1-3.

There are two plankton tow sites in the North Atlantic, one in the Iceland Sea northeast of Iceland (JR271 B6, Table 1) and the other in the Iceland Basin southeast of Iceland (JR271 B5). The closest iodate profiles are from Waite et al. (2006) and we use the North-East station, which was ca. 240 km northwest of our station JR271 B6. In Figure 2C the August 2000 profile from Waite et al. (2006) is shown, as this season matches best with the plankton samples that were taken

in June 2012. Both oxygen and iodate profiles show little vertical variation, with mean iodate values of 410 nmol/l in the upper 150 m and a slight surface reduction to 390 nmol/l. The climatological oxygen concentrations were 200 to 300 $\mu\text{mol/mol}$ (WOA18, Garcia et al., 2019) for both plankton net stations around Iceland.

Water column measurements from Drake Passage were ~ 150 km and ~ 370 km distance away from the plankton tow sites. At this location (59.5°S, 56.5°W) dissolved oxygen concentrations decrease gradually from ~ 330 $\mu\text{mol/kg}$ at the surface to 200 $\mu\text{mol/kg}$ at 1000 m (Figure 2D, WOA18, Garcia et al., 2019). The closest iodate profile is at station PS71/232-1 from Bluhm et al. (2011) and shows slightly lower sea surface iodate concentrations of 330 nmol/l, but uniform further below (350 to 400 nmol/l). Both oxygen and iodate concentrations have similar high values across the whole Drake Passage (Bluhm et al., 2011; Garcia et al., 2019).

Tow-derived planktic foraminifera I/Ca ratios vary between the detection limit of the method (average 0.1 $\mu\text{mol/mol}$) and 0.72 $\mu\text{mol/mol}$, with the lowest values reported for the Northeastern tropical Pacific Site (between detection limit and 0.17 $\mu\text{mol/mol}$), whereas at the Benguela and North and South Atlantic stations they varied between 0.19 $\mu\text{mol/mol}$ and 0.72 $\mu\text{mol/mol}$ (Table 1).

In addition, three species of planktic foraminifera from the South Atlantic ODP core 1088 (0-1 cm, 41.14°S, 13.56°E) were analyzed. They were displaying either semi-transparent tests (fresh) or encrusted white tests (gametogenic and diagenetic overprint). The semi-transparent samples are on average 0.89 ± 0.65 $\mu\text{mol/mol}$ lower than the white specimens at an average I/Ca of 2.89 $\mu\text{mol/mol}$ (Table 3).

Discussion

Seawater oxygen and net haul planktic foraminifera I/Ca ratios

In Figure 3 we compare tow-derived planktic foraminifera I/Ca ratios with *in situ* (i.e., the plankton net depth range) and water column minimum oxygen concentrations to assess whether planktic foraminifera I/Ca ratios reflect redox conditions. There is no relationship between fresh planktic foraminifera I/Ca ratios and *in situ* oxygen concentrations. We note that none of the species analyzed

TABLE 3 I/Ca results of foraminifera with semi-transparent and cloudy appearances from ODP core 1088 (0 to 1 cm).

Species	Semi-transparent specimen I/Ca ($\mu\text{mol/mol}$)	White specimens I/Ca ($\mu\text{mol/mol}$)
<i>Globigerina bulloides</i>	2.42	3.07
<i>Globorotalia truncatulinoides</i>	3.13	4.49 4.66
<i>Globorotalia inflata</i>	3.13	4.12 3.03

have a habitat in the OMZ, as shallower-dwelling species have historically been used for I/Ca reconstructions (Lu et al., 2016b; Hoogakker et al., 2018). However, when we compare planktic foraminifera I/Ca ratios with minimum oxygen concentrations (following Lu et al., 2016a and Lu et al., 2020), then we observe that the lowest I/Ca ratios of $\leq 0.17 \mu\text{mol/mol}$ correspond to the lowest oxygen concentration of $< 10 \mu\text{mol/kg}$, while the other samples are still widely spread (Figure 3). This threshold is much lower than previously observed for core top I/Ca ratios that are generally below $2.5 \mu\text{mol/mol}$ when minimum oxygen concentration is below 50 to $100 \mu\text{mol/kg}$ (Lu et al., 2016a; Lu et al., 2020). The lack of a relationship between planktic foraminifera I/Ca and *in situ* oxygen concentrations could be reflective of the relatively long time of months to years it takes for iodide to be oxidized back to iodate within the oxygenated surface waters overlying oxygen depleted waters (Hardisty et al., 2020 and references therein). At higher oxygen concentrations, between 40 and $300 \mu\text{mol/kg}$, planktic foraminifera I/Ca varies between 0.19 and $0.72 \mu\text{mol/mol}$.

Seawater oxygen, iodate and tow planktic foraminifera I/Ca ratios

This is the first study to compare modern planktic foraminifera I/Ca ratios versus dissolved oxygen and iodate concentrations. It is important to note that we only have *in situ* oxygen and iodate profiles

from the same location as the plankton-tows for the Benguela locations. For the other three locations we used the nearest profiles available from other studies, which were not only sampled during a different year but also at a distance from the tows. As can be seen from Figure 1, the global database for ocean iodine speciation is still very limited in coverage (Chance et al., 2019). Despite relatively sparse observations, large scale latitudinal and depth gradients in iodate abundance are well described (see e.g., Chance et al., 2014), and the profiles we have selected for comparison are consistent with these trends. We compare our North Atlantic plankton tow samples with the iodate and oxygen profiles of station “NE” from Waite et al. (2006), ca. 240 km northwest of our station JR271 B6. Waite et al. (2006) found iodine speciation in this region to be spatially and temporally stable – iodate profiles were very similar ($> 400 \text{ nmol/L}$ throughout the top 1000 m) to the NE station at additional stations four degrees further south (“SW”) and 15 degrees further west (“NW”), and showed very little variation between November, February, and August. For the NE Pacific, iodate and supporting oxygen profiles are from a location to the south of the plankton tow (distance 400 km). However, with iodate in subsurface and mixed layer water being quite variable in the Pacific (Rue et al., 1997; Cutter et al., 2018; Moriyasu et al., 2020), we are constrained in our comparison of seawater iodate concentrations with planktic foraminifera I/Ca ratios. Below $\sim 300 \text{ m}$, all four locations show uniform 400 nmol/L , whilst oxygen concentrations vary considerably (Figure 2). In the top 300 m there are some notable differences, with

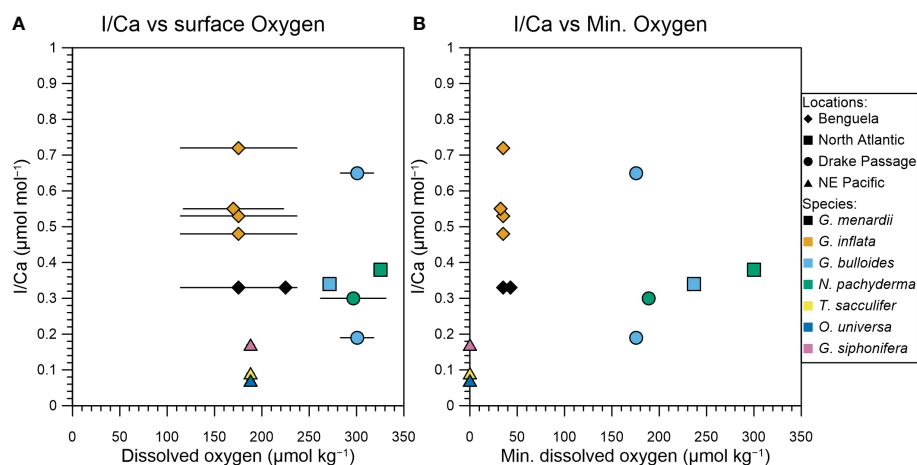


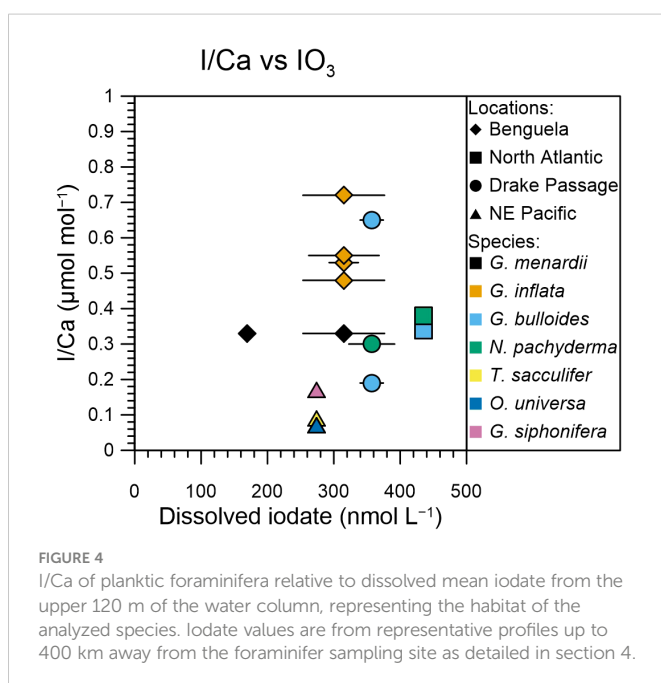
FIGURE 3

I/Ca values of planktic foraminifera compared to seawater oxygen concentrations. (A) planktic foraminifera I/Ca from net hauls vs. mean oxygen concentrations from the upper 120 m from nearby CTD casts. The range shows the maximum and minimum oxygen concentrations in the upper 120 m. (B) planktic foraminifera I/Ca vs. the minimum water column oxygen concentration, generally deeper down in the water column.

the NE Pacific showing a large reduction in iodate when oxygen levels fall below 5 $\mu\text{mol/kg}$.

In surface waters oxygen concentrations are influenced by primary production, temperature, remineralization of organic material, and mixing with other water masses. The distribution of iodide and iodate in the oxygenated ocean is thought to arise from the interplay of the biologically mediated transformations, and physical mixing and advection processes (Campos et al., 1996; Truesdale and Bailey, 2000; Chance et al., 2014). In areas where oxygen is severely depleted, such as subsurface oxygen minimum zones, iodide becomes the dominant form of iodine (e.g., Wong and Brewer, 1977; Wong et al., 1985; Rue et al., 1997; Truesdale and Bailey, 2000). It appears that iodate becomes depleted, and iodide the dominant iodine species when oxygen concentrations fall below $7 \pm 2 \mu\text{mol/kg}$ (Rue et al., 1997; Cutter et al., 2018; Moriyasu et al., 2020). It is only in the NE Pacific that oxygen reaches such low levels (Figure 2).

Comparison of our planktic foraminifera I/Ca ratios with seawater dissolved iodate does not show a very clear relationship (Figure 4). We use the depth range of the nets to calculate a vertically weighted mean iodate concentration. In the top 120 m of the well-oxygenated North and South Atlantic the mean iodate concentrations are slightly elevated (310–360 nmol/l) compared to the Benguela and NE Pacific (210–340 nmol/l). While the iodate profiles in the top 120 m at Benguela and the NE Pacific look similar, the planktic foraminifera from the NE Pacific have lower I/Ca values compared with those from the Benguela sites (Figure 4). Unless *in situ* seawater iodate values at the NE Pacific sites are lower than measured for station 19 ~400 km away from the site, these results suggest that the relationship between planktic foraminifera I/Ca and seawater iodate concentration may not be straightforward. More contemporary data containing planktic foraminifera I/Ca and seawater iodate concentrations are needed to improve our understanding of the use of planktic foraminifera I/Ca as a potential subsurface redox proxy.



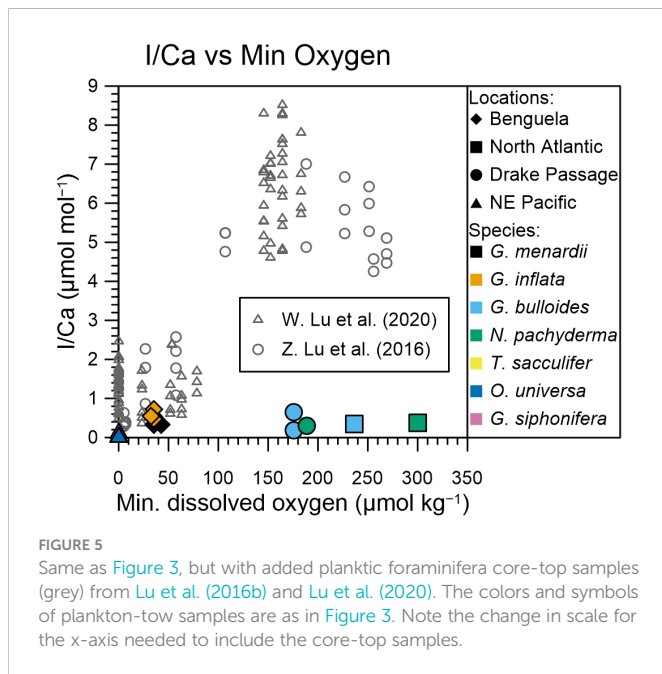
Comparison of plankton tow derived planktic foraminifera I/Ca with core-tops

There are various proxies that have been used to capture low oxygen waters of OMZs: presence/absence of sedimentary laminations, benthic foraminifera assemblages and morphology, redox sensitive metals, and nitrogen isotopes (Moffitt et al., 2015; Rathburn et al., 2018; Erdem et al., 2020; Studer et al., 2021). Application of most of these proxies are however limited to sediment cores that are immersed in low oxygen waters (Winkelbauer et al., 2021), limiting the areal extent of assessments of past OMZs to the upper continental slope. Iodine/calcium ratios, measured in planktic foraminifera that calcified in close proximity of the OMZ (e.g., in seawater directly within or above it) have the potential to expand research on seawater redox conditions to the open ocean (Winkelbauer et al., 2021), as do planktic-foraminifera shell-bound nitrogen isotopes (Smart et al., 2020; Studer et al., 2021). Any downcore application of such proxies needs calibration whether quantitative or qualitative.

Core-top planktic foraminifera I/Ca data can be divided into two groups: those with I/Ca ratios of $> 4 \mu\text{mol/mol}$, which appear to be characteristic of areas where minimum dissolved oxygen concentrations are between 100 and 280 $\mu\text{mol/mol}$; and those with $I/Ca < 2.5 \mu\text{mol/mol}$, which appear to be characteristic of areas where minimum subsurface oxygen concentrations are below 90 $\mu\text{mol/mol}$ (Figure 5, Lu et al., 2016a; Lu et al., 2020). These authors compared their planktic foraminifera I/Ca data with the lowest oxygen concentrations in the water column, which does not generally represent the water depth that the foraminifera calcify at. For example, for the North-East Pacific, Davis et al. (2021) show that only a few planktic foraminifera species, like *Globorotaloides hexagonus*, are found in very low oxygen environments, whereas most species are found in the well-oxygenated mixed layer. Lu et al. (2020) argue that minimum water column oxygen concentrations need to be used as the oxygen content must drop below a certain threshold to trigger iodate reduction, which then gets recorded as low foraminiferal I/Ca (Lu et al., 2016a). Seawater iodate generally starts to reduce under suboxic conditions ($O_2 < 10 \mu\text{mol/kg}$), so a low I/Ca ratio $< 1 \mu\text{mol/mol}$ in our planktic foraminifera samples cannot be explained by iodate reduction when the minimum oxygen concentration is $> 100 \mu\text{mol/kg}$ (Figure 5).

Another important question is how signals from the OMZ/ oxygen depleted waters are communicated to planktic foraminifera living in the generally shallower and better oxygenated mixed layer. Potentially, this could be related to the time it takes for iodide to oxidize to iodate, where in settings with suboxia in subsurface waters the iodate concentration of the mixed layer above is decreased as a result of vertical exchange compared to settings with a mildly hypoxic or well oxygenated water column. More research is needed to explore this.

It is striking that across the spectrum of dissolved oxygen concentrations planktic foraminifera I/Ca ratios from core-tops are significantly higher than tow-derived samples (Figure 5). In OMZ environments, core-top samples show considerable variation, with I/Ca ratios between the detection limit and 2.5 $\mu\text{mol/mol}$; whereas plankton tow samples are limited to 0.17 $\mu\text{mol/mol}$. Furthermore, core-top planktic foraminifera I/Ca ratios from



better oxygenated environments (>100 $\mu\text{mol/kg}$) show values between 4 and 9 $\mu\text{mol/mol}$; plankton tows only reach 0.72 $\mu\text{mol/mol}$ (Figure 5).

Our observations of an order of magnitude lower I/Ca ratios in planktic foraminifera from plankton tows compared with core-tops would suggest that planktic foraminifera gain iodine post-mortem. This could be *via* abiotic incorporation shortly after gametogenesis, or when sinking through the water column, or following burial because the bottom waters were better ventilated with high iodate concentrations. Post depositional crust formation has been observed in planktic foraminifera with the potential to affect paleoproxy records of Mg/Ca and Sr/Ca (Branson et al., 2015). Diagenetic processes could also influence the I/Ca ratio of foraminifera tests, depending on the iodate concentration of the pore water. Throughout their lifecycle, planktic foraminifera migrate vertically through the water column. At the end of their lifecycle, prior to or during gametogenesis, various species form a calcite crust, which can potentially account for most of the total shell mass. Gametogenic crusts can dominate the element signature of the shell (Steinhardt et al., 2015). Steinhardt et al. (2015) show that planktic foraminifera Mg/Ca ratios of *N. dutertrei* and *G. scitula* are significantly lower (50%) in the crust compared with ontogenic calcite. Incorporation of iodate seems to be higher in abiotic calcification (Lu et al., 2010) compared to biotic calcification of foraminifera (Figure 5), therefore, abiotic crust growth in the sediments can increase the overall I/Ca of foraminifera after deposition. If crust also plays a role in planktic foraminifera I/Ca ratios, then the results shown here (Figure 5) would suggest that crust addition in well-oxygenated settings causes a 5 to 11 times increase in I/Ca ratios, whereas in lower oxygenated settings this is reduced (in case of suboxic water column) or is negligible (in case of mild hypoxia in the water column). However, we do not univocally observe a greater I/Ca enrichment in species that form a thicker crust, like *N. dutertrei* or *N. pachyderma* (Lu et al., 2016a; Hoogakker et al., 2018; Lu et al., 2020).

To further assess the potential effect of crusts on planktic foraminifera I/Ca ratios, we measured I/Ca ratios for *G. bulloides*, *G. truncatulinoides* and *G. inflata* samples from ODP Site 1088 (0–1 cm), comparing heavily encrusted samples with those that were transparent to semi-transparent (i.e., limited encrustation). *Globigerina bulloides* does not form a crust to the degree that *G. truncatulinoides* and *G. inflata* do in the water column such that most overgrowth in this species should happen after sedimentation at the seafloor. While the transparent samples did not show similar values as the plankton tows (e.g., below 1 $\mu\text{mol/mol}$) their I/Ca ratios were lower compared to those that showed considerable encrustation (Table 3). This supports our hypothesis that in higher oxygenated settings crusts are associated with increased I/Ca ratios of core-top planktic foraminifera.

Conclusions

Here we compared planktic foraminifera I/Ca ratios, obtained from plankton tows, with published and new measurements of seawater iodate and oxygen concentrations from 1) the Eastern North Pacific with extensive oxygen depletion, 2) the Benguela Current System with moderately depleted oxygen concentrations, and 3) the well oxygenated North and South Atlantic. While we do not observe a clear relationship between seawater iodate concentration in the upper 120 m and planktic foraminifera I/Ca, we do find that the lower planktic foraminifera I/Ca ratios are found in areas characterized by depleted oxygen concentrations in subsurface waters at 430 m. The observed trend is similar to that of core-top studies, however, plankton-tow derived samples from well-oxygenated regions have I/Ca ratios that are an order of magnitude lower than their core-top counterparts. We suggest that planktic foraminifera may gain iodine prior to or following gametogenesis or post-mortem, at least in well-oxygenated areas, either when falling through the water column, or through burial.

Data availability statement

The original contributions presented in the study are included in the article/Supplementary Material. Further inquiries can be directed to the corresponding authors.

Author contributions

HW and BH have created the concept and design of the study. HW, BH, EH, SC, and PH have conducted the I/Ca analysis. HW has prepared figures and managed the data. BH and HW have contributed to writing the first draft of the manuscript. RC, CD, LC, SC, PH, AP, and KW have commented on the first draft of the manuscript. RC, LC, and CA have organized and conducted the analysis of seawater iodate concentrations in York. RC has curated the global iodate data. KW has collected the plankton samples on cruise SKQ2017 and CD picked them. JB contributed to the sample preparation in the Lyell Centre. VP collected plankton samples on cruises JR271 and JR274. HW and AP contributed to sampling iodate

water samples and plankton samples on cruise DY090. MS analyzed oxygen samples on cruise DY090. KW has taken plankton samples and provided sensor data on cruise SKQ2017. All authors contributed to the article and approved the submitted version.

Funding

This work was supported by a James Watt Scholarship awarded to HW. BH acknowledges support from UKRI Future Leaders Grant MR/S034293/1 and UK Natural Environment Research Council (NERC) grant NE/I020563/1. RC and LC profited from NERC grant NE/N009983/1 (Iodide in the ocean: distribution and impact on iodine flux and ozone loss) and NE/W00027X/1 (Iodine sea-air emissions and atmospheric impacts in a changing world (I-SEA)). Collection of the foraminifera specimens (by the MOCNESS net) in the Eastern Tropical Pacific OMZ during two research cruises was funded by National Science Foundation grant OCE-1459243 (PIs were Seibel, Wishner, and Roman). United States National Science Foundation OCE-1851589 to CD was used to support the isolation of foraminifera from MOCNESS tows in the Eastern Tropical North Pacific. The Benguela Cruise “COMICS” was funded by NERC with the codes NE/M020835/1 and NE/M020835/2. VP benefited from the UK Ocean Acidification research programme which was funded by the Department for Environment, Food and Rural Affairs, the NERC and the Department of Energy and Climate Change (NE/H017267/1, NE/H017097/1).

Acknowledgments

The authors thank the crews and scientific team of the *R/V Sikuliaq* SKQ201701S, *RRS Discovery* DY090 and *James Clark Ross* JR271 and JR274 cruises for help with the sample acquisition. Joe

References

- Anand, P., Elderfield, H., and Conte, M. H. (2003). Calibration of Mg/Ca thermometry in planktonic foraminifera from a sediment trap time series. *Paleoceanography* 18 (2):1050. doi: 10.1029/2002PA000846
- Bluhm, K., Croot, P. L., Huhn, O., Rohardt, G., and Lochte, K. (2011). Distribution of iodide and iodate in the Atlantic sector of the southern ocean during austral summer. *Deep Sea Res. Part II: Topical Stud. Oceanogr.* 58 (25–26), 2733–2748. doi: 10.1016/j.dsr2.2011.02.002
- Boyer, T. P., Garcia, H., Locarnini, R., Zweng, M., Mishonov, A., Reagan, J., et al. (2018). *World ocean atlas 2018 [temperature, oxygen and nitrate subsets]* (NOAA National Centers for Environmental Information). <https://www.ncei.noaa.gov/archive/accession/NCEI-WOA18>
- Branson, O., Read, E., Redfern, S. A., Rau, C., and Elderfield, H. (2015). Revisiting diagenesis on the ontong Java plateau: Evidence for authigenic crust precipitation in globorotalia tumida. *Paleoceanography* 30 (11), 1490–1502. doi: 10.1002/2014PA002759
- Breitbart, D., Levin, L. A., Oschlies, A., Grégoire, M., Chavez, F. P., Conley, D. J., et al. (2018). Declining oxygen in the global ocean and coastal waters. *Sci. (New York N.Y.)* 359 (6371):eaam7240. doi: 10.1126/science.aam7240
- Buchwald, C., Santoro, A. E., Stanley, R. H. R., and Casciotti, K. L. (2015). Nitrogen cycling in the secondary nitrite maximum of the eastern tropical north pacific off Costa Rica. *Global Biogeochem. Cycles* 29 (12), 2061–2081. doi: 10.1002/2015GB005187
- Campos, M. L. A. M. (1997). New approach to evaluating dissolved iodine speciation in natural waters using cathodic stripping voltammetry and a storage study for preserving iodine species. *Mar. Chem.* 57 (1–2), 107–117. doi: 10.1016/S0304-4203(96)00093-X
- Campos, M. L. A. M., Farrenkopf, A. M., Jickells, T. D., and Luther, G. W. III (1996). A comparison of dissolved iodine cycling at the Bermuda Atlantic time-series station and Hawaii ocean time-series station. *Deep Sea Res. Part II: Topical Stud. Oceanogr.* 43 (2–3), 455–466. doi: 10.1016/0967-0645(95)00100-X
- Chai, J. Y., and Muramatsu, Y. (2007). Determination of bromine and iodine in twenty-three geochemical reference materials by ICP-MS. *Geostandards Geoanalytical Res.* 31 (2), 143–150. doi: 10.1111/j.1751-908X.2007.00856.x
- Chance, R., Baker, A. R., Carpenter, L. J., and Jickells, T. D. (2014). The distribution of iodide at the sea surface. *Environ. Sci.: Processes Impacts* 16 (8), 1841–1859. doi: 10.1039/C4EM00139G
- Chance, R., Tinel, L., Sherwen, T., Baker, A. R., Bell, T., Brindle, J., et al. (2019). Metadata record for: Global sea-surface iodide observations *ScientificData* 6 1967–2018. doi: 10.6084/M9.FIGSHARE.10130129
- Cutter, G. A., Moffett, J. W., Nielsdóttir, M. C., and Sanial, V. (2018). Multiple oxidation state trace elements in suboxic waters off Peru: *In situ* redox processes and advective/diffusive horizontal transport. *Mar. Chem.* 201, 77–89. doi: 10.1016/j.marchem.2018.01.003
- Davis, C. V., Wishner, K., Renema, W., and Hull, P. M. (2021). Vertical distribution of planktic foraminifera through an oxygen minimum zone: how assemblages and test morphology reflect oxygen concentrations. *Biogeosciences* 18 (3), 977–992. doi: 10.5194/bg-18-977-2021
- Erdem, Z., Schönfeld, J., Rathburn, A. E., Pérez, M.-E., Cardich, J., and Glock, N. (2020). Bottom-water deoxygenation at the Peruvian margin during the last deglaciation recorded by benthic foraminifera. *Biogeosciences* 17 (12), 3165–3182. doi: 10.5194/bg-17-3165-2020
- Evans, N., Boles, E., Kwiecinski, J. V., Mullen, S., Wolf, M., Devol, A. H., et al. (2020). The role of water masses in shaping the distribution of redox active compounds in the

Install and Rhianna Evans are thanked for their contributions to iodate water sample analysis.

Conflict of interest

The authors declare that the research was conducted in the absence of any commercial or financial relationships that could be construed as a potential conflict of interest.

Publisher's note

All claims expressed in this article are solely those of the authors and do not necessarily represent those of their affiliated organizations, or those of the publisher, the editors and the reviewers. Any product that may be evaluated in this article, or claim that may be made by its manufacturer, is not guaranteed or endorsed by the publisher.

Supplementary material

The Supplementary Material for this article can be found online at: <https://www.frontiersin.org/articles/10.3389/fmars.2023.1095570/full#supplementary-material>

SUPPLEMENTARY FIGURE 1

CTD bottle profiles of iodate (circles) and dissolved oxygen (diamonds) concentrations from the station South Benguela.

SUPPLEMENTARY FIGURE 2

CTD bottle profiles of iodate (circles) and dissolved oxygen (diamonds) concentrations from the station North Benguela.

SUPPLEMENTARY FIGURE 3

More CTD bottle profiles of iodate (circles) and dissolved oxygen (diamonds) concentrations from the station North Benguela.

Eastern tropical north pacific oxygen deficient zone and influencing low oxygen concentrations in the eastern pacific ocean. *Limnol. Oceanogr.* 65 (8), 1688–1705. doi: 10.1002/lno.11412

Feng, X., and Redfern, S. A. T. (2018). Iodate in calcite, aragonite and vaterite CaCO₃: Insights from first-principles calculations and implications for the I/Ca geochemical proxy. *Geochimica Et Cosmochimica Acta* 236, 351–360. doi: 10.1016/j.gca.2018.02.017

García, H. E., Weathers, K. W., Paver, C. R., Smolyar, I., Boyer, T. P., Locarnini, M. M., et al. (2019). “World ocean atlas 2018,” in *Dissolved oxygen, apparent oxygen utilization, and dissolved oxygen saturation* NOAA Atlas NESDIS 3,83 38. <https://archimer.ifremer.fr/doc/00651/76337>

Garfield, P. C., Packard, T. T., Friederich, G. E., and Codispoti, L. A. (1983). A subsurface particle maximum layer and enhanced microbial activity in the secondary nitrite maximum of the northeastern tropical pacific ocean. *J. Mar. Res.* 41 (4), 747–768. doi: 10.1357/002224083788520496

Glock, N., Liebetrau, V., and Eisenhauer, A. (2014). I/Ca ratios in benthic foraminifera from the Peruvian oxygen minimum zone: analytical methodology and evaluation as a proxy for redox conditions. *Biogeosciences* 11 (23), 7077–7095. doi: 10.5194/bg-11-7077-2014

Glock, N., Liebetrau, V., Eisenhauer, A., and Rocholl, A. (2016). High resolution I/Ca ratios of benthic foraminifera from the Peruvian oxygen–minimum–zone: A SIMS derived assessment of a potential redox proxy. *Chem. Geology* 447, 40–53. doi: 10.1016/j.chemgeo.2016.10.025

Hardisty, D. S., Horner, T. J., Wankel, S. D., Blusztajn, J., and Nielsen, S. G. (2020). Experimental observations of marine iodide oxidation using a novel sparge–interface MC-ICP-MS technique. *Chem. Geology* 532, 119360. doi: 10.1016/j.chemgeo.2019.119360

Hoogakker, B. A. A., Lu, Z., Umling, N., Jones, L., Zhou, X., Rickaby, R. E. M., et al. (2018). Glacial expansion of oxygen-depleted seawater in the eastern tropical pacific. *Nature* 562 (7727), 410–413. doi: 10.1038/s41586-018-0589-x

Jickells, T. D., Boyd, S. S., and Knap, A. H. (1988). Iodine cycling in the Sargasso Sea and the Bermuda inshore waters. *Mar. Chem.* 24 (1), 61–82. doi: 10.1016/0304-4203(88)90006-0

Lu, W., Dickson, A. J., Thomas, E., Rickaby, R. E., Chapman, P., and Lu, Z. (2020). Refining the planktic foraminiferal I/Ca proxy: Results from the southeast Atlantic ocean. *Geochimica Cosmochimica Acta* 287, 318–327. doi: 10.1016/j.gca.2019.10.025

Lu, Z., Hoogakker, B. A. A., Hillenbrand, C.-D., Zhou, X., Thomas, E., Gutchess, K. M., et al. (2016a). Oxygen depletion recorded in upper waters of the glacial southern ocean. *Nat. Commun.* 7, 11146. doi: 10.1038/ncomms11146

Lu, Z., Hoogakker, B. A. A., Hillenbrand, C.-D., Zhou, X., Thomas, E., Gutchess, K. M., et al. (2016b). “Oxygen depletion recorded in upper waters of the glacial southern ocean,” in *(Table S1) I/Ca ratios of surface sediments (PANGAEA)*. doi: 10.1594/PANGAEA.869449

Lu, Z., Jenkyns, H. C., and Rickaby, R. E. M. (2010). Iodine to calcium ratios in marine carbonate as a paleo-redox proxy during oceanic anoxic events. *Geology* 38 (12), 1107–1110. doi: 10.1130/G31145.1

Medina Faull, L., Mara, P., Taylor, G. T., and Edgcomb, V. P. (2020). Imprint of trace dissolved oxygen on prokaryoplankton community structure in an oxygen minimum zone. *Front. Mar. Sci.* 7 (360). doi: 10.3389/fmars.2020.00360

Moffitt, S. E., Moffitt, R. A., Sauthoff, W., Davis, C. V., Hewett, K., and Hill, T. M. (2015). Paleooceanographic insights on recent oxygen minimum zone expansion: Lessons for modern oceanography. *PLoS One* 10 (1), e0115246. doi: 10.1371/journal.pone.0115246

Moriyasu, R., Evans, Z. C., Bolster, K. M., Hardisty, D. S., and Moffett, J. W. (2020). The distribution and redox speciation of iodine in the Eastern tropical north pacific ocean. *Global Biogeochem. Cycles* 34 (2):e2019GB00630. doi: 10.1029/2019GB006302

Orsi, A. H., Whitworth, III, T., and Nowlin, J. W.D. (1995). On the meridional extent and fronts of the Antarctic circumpolar current. *Deep Sea Res. Part I: Oceanographic Res. Papers* 42 (5), 641–673. doi: 10.1016/0967-0637(95)00021-W

Oschlies, A., Schulz, K. G., Riebesell, U., and Schmittner, A. (2008). Simulated 21st century’s increase in oceanic suboxia by CO₂-enhanced biotic carbon export. *Global Biogeochem. Cycles* 22 (4):467–473. doi: 10.1029/2007GB003147

Podder, J., Lin, J., Sun, W., Botis, S. M., Tse, J., Chen, N., et al. (2017). Iodate in calcite and vaterite: Insights from synchrotron X-ray absorption spectroscopy and first-principles calculations. *Geochimica Et Cosmochimica Acta* 198, 218–228. doi: 10.1016/j.gca.2016.11.032

Rathburn, A. E., Willingham, J., Ziebis, W., Burkett, A. M., and Corliss, B. H. (2018). A new biological proxy for deep-sea paleo-oxygen: Pores of epifaunal benthic foraminifera. *Sci. Rep.* 8 (1), 9456. doi: 10.1038/s41598-018-27793-4

Rue, E. L., Smith, G. J., Cutter, G. A., and Bruland, K. W. (1997). The response of trace element redox couples to suboxic conditions in the water column. *Deep Sea Res. Part I: Oceanographic Res. Papers* 44 (1), 113–134. doi: 10.1016/S0967-0637(96)00088-X

Schlitzer, R. (2022) *Ocean data view*. Available at: <https://odv.awi.de>.

Schwehr, K. A., and Santschi, P. H. (2003). Sensitive determination of iodine species, including organo-iodine, for freshwater and seawater samples using high performance liquid chromatography and spectrophotometric detection. *Analytica Chimica Acta* 482 (1), 59–71. doi: 10.1016/S0003-2670(03)00197-1

Smart, S. M., Fawcett, S. E., Ren, H., Schiebel, R., Tompkins, E. M., Martínez-García, A., et al. (2020). The nitrogen isotopic composition of tissue and shell-bound organic matter of planktic foraminifera in southern ocean surface waters. *Geochem. Geophysics Geosystems* 21 (2):e2019GC008440. doi: 10.1029/2019GC008440

Steinhardt, J., de Nooijer, L. J., Brummer, G.-J.A., and Reichart, G.-J. (2015). Profiling planktonic foraminiferal crust formation. *Geochem. Geophysics Geosystems* 16 (7), 2409–2430. doi: 10.1002/2015GC005752

Studer, A. S., Mekik, F., Ren, H., Hain, M. P., Oleynik, S., Martínez-García, A., et al. (2021). Ice Age–Holocene similarity of Foraminifera–Bound nitrogen isotope ratios in the Eastern equatorial pacific. *Paleoceanogr. Paleoclimatol.* 36 (5):e2020PA004063. doi: 10.1029/2020PA004063

Truesdale, V. W., and Bailey, G. W. (2000). Dissolved iodate and total iodine during an extreme hypoxic event in the southern benguela system. *Estuarine Coast. Shelf Sci.* 50 (6), 751–760. doi: 10.1006/ecss.2000.0609

Truesdale, V. W., Bale, A., and Woodward, E. (2000). The meridional distribution of dissolved iodine in near-surface waters of the Atlantic ocean. *Prog. Oceanogr.* 45 (3–4), 387–400. doi: 10.1016/S0079-6611(00)00009-4

Truesdale, V. W., and Spencer, C. P. (1974). Studies on the determination of inorganic iodine in seawater. *Mar. Chem.* 2 (1), 33–47. doi: 10.1016/0304-4203(74)90004-8

Veitch, J. A., Florenchie, P., and Shillington, F. A. (2006). Seasonal and interannual fluctuations of the Angola–benguela frontal zone (ABFZ) using 4.5 km resolution satellite imagery from 1982 to 1999. *Int. J. Remote Sens.* 27 (5), 987–998. doi: 10.1080/01431160500127914

Waite, T. J., Truesdale, V. W., and Olafsson, J. (2006). The distribution of dissolved inorganic iodine in the seas around Iceland. *Mar. Chem.* 101 (1–2), 54–67. doi: 10.1016/j.marchem.2006.01.003

Winkelbauer, H., Cordova-Rodriguez, K., Reyes-Macaya, D., Scott, J., Glock, N., Lu, Z., et al. (2021). Foraminifera iodine to calcium ratios: approach and cleaning. *Geochem. Geophysics Geosystems* 22, 1–11. doi: 10.1029/2021GC009811

Wishner, K. F., Seibel, B. A., Roman, C., Deutsch, C., Outram, D., Shaw, C. T., et al. (2018). Ocean deoxygenation and zooplankton: Very small oxygen differences matter. *Sci. Adv.* 4 (12), eaau5180. doi: 10.1126/sciadv.aau5180

Wong, G. T., and Brewer, P. G. (1977). The marine chemistry of iodine in anoxic basins. *Geochimica Et Cosmochimica Acta* 41 (1), 151–159. doi: 10.1016/0016-7037(77)90195-8

Wong, G. T., Takayanagi, K., and Todd, J. F. (1985). Dissolved iodine in waters overlying and in the orca basin, gulf of Mexico. *Mar. Chem.* 17 (2), 177–183. doi: 10.1016/0304-4203(85)90072-6

Zhang, S., Xu, C., Creeley, D., Ho, Y.-F., Li, H.-P., Grandbois, R., et al. (2013). Iodine-129 and iodine-127 speciation in groundwater at the hanford site, US: Iodate incorporation into calcite. *Environ. Sci. Technol.* 47 (17), 9635–9642. doi: 10.1021/es401816e